A theory for the impact of a wave breaking onto a permeable barrier with jet generation

Mark J. Cooker
School of Mathematics, University of East Anglia, Norwich NR4 7TJ, UK
Email: m.cooker@uea.ac.uk Tel +44 (01603) 592 975 Fax +44 (01603) 593 868

Submitted to J. Eng. Math. 12th October 2011 Accepted 9 May 2012

Abstract. We model a water wave impact onto a porous breakwater. The breakwater surface is modelled as a thin barrier composed of solid matter pierced by channels through which water can flow freely. The water in the wave is modelled as a finite-length volume of inviscid, incompressible fluid in quasi-one-dimensional flow during its impact and flow through a typical hole in the barrier. The fluid volume moves at normal incidence to the barrier. After the initial impact the wave water starts to slow down as it passes through holes in the barrier. Each hole is the source of a free jet along whose length the fluid velocity and width vary in such a way as to conserve volume and momentum at zero pressure. We find there are two types of flow, depending on the porosity, β, of the barrier. If $\beta : 0 \leq \beta < 0.5774$ then the barrier is a strong impediment to the flow, in that the fluid velocity tends to zero as time tends to infinity. But if $\beta : 0.5774 \leq \beta \leq 1$ then the barrier only temporarily holds up the flow, and the decelerating wave water passes through in a finite time. We report results for the velocity and impact pressure due to the incident wave water, and for the evolving shape of the jet, with examples from both types of impact. We account for the impulse on the barrier and the conserved kinetic energy of the flow. Consideration of small β gives insight into the sudden changes in flow and the high pressures that occur when a wave impacts a nearly impermeable seawall.

Keywords: wave impact pressures; jet; porous structure

1. Introduction

Sudden, large and rapidly changing forces are exerted by steep sea waves when they break against coastal structures. For a rubble mound breakwater the seaward boundary is a surface composed of impermeable rock interspersed with holes that allow ready penetration of the structure by wave water. The holes are entries to passageways and voids between the blocks, boulders or concrete elements that make up the structure. Even a monolithic vertical breakwater may contain cracks or spaces between the masonry blocks that allow high-speed water entry from breaking-wave impact. A wave that overturns and breaks onto a steep shingle beach (common in the British Isles) encounters a very open surface, able to admit a large fraction of the wave water before its seaward backwash occurs. In order to understand these forces we need first to model the time-dependent pressure distribution associated with the flow arriving on the seaward boundary of the structure. It is only by modelling the time-dependent flow, as the wave penetrates the outermost layer of rock, that we can hope to understand the impact pressures, and learn something of the starting conditions for the subsequent flow deeper into the structure. This paper is mostly about the flow in the wave and its transformation into free jets that shoot inside the labyrinth of a rubble mound breakwater or shingle. The free jets go on to cross the void spaces and collide with the faces of the interior rock. However, these internal collisions are local events that do not have upstream influence on the flow conditions that we model in the region close to the structure's surface.

Bagnold [1] was one of the first to treat water wave impact mechanics in terms of the sudden changes that occur in the momentum of the fluid during impact against a wall. Other pioneering work on the analysis of steady jets was carried out by Taylor [15] who modelled the flow in a shaped charge. Further details are found in Birkhoff *et al.* [2] and

the first four chapters of Birkhoff and Zarantonello [3]. In these studies and the present paper, the Reynolds number and the Froude number are both so high that viscosity and gravity are negligible.

If a liquid region with a free surface falls onto a rigid impermeable plane, then, soon after contact, liquid jets spread laterally over the plane. These fast jets are difficult to analyse or resolve adequately in computations. The fluid domain near the site of impact is greatly extended by the jet flow, and there are accelerations of thousands of g to be accounted for in the early stages after impact. Segments of the free surface, which are initially short, quickly become elongated by the flow. In a computation the free surface (and its velocity field) may become unacceptably poorly resolved in space and time. Korobkin and Yilmaz [12], model a similar situation for a dam-break flow, where a horizontal jet emerges near the bed. Splash jets also occur in the water entry of a solid body. These have been analysed for a blunt body by Howison *et al.* [9]. Part of their analysis uses the theory of Wagner [17] for describing the position and nature of the overturning free surface near the jet root, theory which is explained further in chapter 9 of Faltinsen [8]. The splash jets made by droplet impact onto a liquid layer are treated by Howison *et al.* [10].

An ascending splash jet can be made by a vertical wavemaker in a water wave tank. King and Needham [11] showed, using small-time asymptotics, that a vertical section of wall, moving horizontally from rest with uniform acceleration into water, also initially at rest, induces an ascending splash-jet whose width and relatively tall vertical displacement both grow from zero. King and Needham [11] solved the problem for an initial fluid domain which is a quarter-plane. Needham *et al.* [13] have treated the jet generated in finite depth by an inclined accelerating plate, including the influences of gravity and surface tension.

Cooker [6] and [7] has modelled the pressures at the early stages of jet growth, in two-dimensional and axisymmetrically converging flows. That earlier work concentrates on the period of time of highest pressure and limited free-surface displacement for the fluid nearest the plane wall being struck. By contrast, the current work focusses on the flow through a sharply defined channel, describing the surface layer of a permeable wave barrier. Violent flows adjacent to and inside a permeable barrier were discussed by Wood and Peregrine [18]. Here, we propose a treatment that is quasi-one-dimensional on an axis perpendicular to the seawall and describes the detailed development in time of the incident flow and jet generation.

The formulations of the governing equations and boundary conditions are developed in §2. The solutions for the flow in the volume of fluid in the wave are worked out in §3. The solutions for the flow in the jet are presented in parametric form in §4. In §5 we describe an example of the kind of calculation that may be made from the theory, relevant to seawave impact. In §6 we report on the energy change in the flow, and we discuss the findings to motivate future work.

2. Analysis

The general arrangement is drawn in Fig. 1. The water in the breaking wave is on the left and the flow is to the right, parallel to the x-axis. The permeable barrier is shown as shaded triangles. The array of jets emerges to the right of the barrier. We treat the wave-water flow and the jet flow separately in the following subsections. The Appendix explains how it is that we may treat the thin barrier between $-W \leq x \leq 0$ as a surface of spatial discontinuity, at $x = 0$, for the pressure and velocity.

2.1. Flow in the incident wave

The fluid is inviscid and incompressible with constant density ϱ. The velocity field is irrotational and may be described by a velocity potential $\phi(x, y, z, t)$, where x, y, z are cartesian coordinates in the inertial frame of reference of the plane barrier, and t is time. The positive x-axis points into the barrier orthogonally, and the thin barrier is at $x = 0$. The wave water first meets the barrier with given speed u_{10} at time $t = 0$. Initially the fluid occupies the region $x : -L_0 \leq x \leq 0$ where the initial length of the wave water is L_0. The velocity field is assumed to be essentially one dimensional and, owing to the fluid's incompressibility, its velocity is spatially uniform: $u_1(t)\mathbf{i}$, where the subscript 1 refers to the region $-L_0 \leq x \leq 0$. In the subsequent motion we suppose that the rear face $x = -L(t)$ of the wave water is a free surface on which the pressure is zero (atmospheric reference). So we have the following kinematic condition at $x = -L$:

$$-\frac{dL}{dt} = u_1(t). \tag{1}$$

The pressure $p_1(x, t)$ and the velocity are governed by the x-component of Euler's equation:

$$\frac{du_1}{dt} = -\frac{1}{\varrho}\frac{\partial p_1}{\partial x}. \tag{2}$$

Integrating (2) in space we have an expression for the pressure, which satisfies the dynamic condition $p_1 = 0$ at the rear of the wave water:

$$p_1(x, t) = -\varrho\,(x + L(t))\frac{du_1}{dt}. \tag{3}$$

2.2. Flow in the hole and into the jet

As the fluid meets the barrier it passes through holes and forms free jets, shown on the right in Fig. 1. We treat the holes as having a cross-sectional area that decreases in the direction of fluid flow. In practical terms the wave water that passes through a hole between elements in a breakwater will continue until it detaches from the interior walls of the hole, so that a free surface is formed downstream. The point of free-surface separation may coincide with the cross-section of the hole which has the smallest area. A pressure gradient is found between the high-pressure at the entrance to each hole and the zero-pressure condition in the jet that emerges at the hole's exit. The pressure gradient accelerates the fluid from the front face of the barrier through the constriction towards the narrower exit. In the Appendix we model this local flow in more detail in order to show that we may simplify its influence to discontinuities in pressure and flow speed across a *thin* barrier, between $x = 0^-$ and $x = 0^+$.

We consider part of the barrier's face, at $x = 0^-$, this forms one facet of a control volume for a region of fluid in $x < 0$ that is able to flow through one typical hole. We assume that this control volume is a prism whose cross-sections share the same area A_1. Now at $x = 0^+$ the hole has an exit of cross-sectional area $A_{20} \leq A_1$. The subscript 2 refers to the region $x \geq 0$ and the subscript 0 refers to $x = 0^+$. The porosity β defined by $\beta = A_{20}/A_1$ is a material constant for the barrier which has a homogeneous array of holes. Naturally between the extremes of impermeable and wholly open, the barrier has a porosity in the interval $0 \leq \beta \leq 1$.

In the short time scale of impact we expect the fluid to pass through the hole so that volume continuity can be appealed to: the equal volume fluxes entering and leaving the hole are related by

$$u_1(t)A_1 = u_{20}(t)A_{20}, \tag{4}$$

where $u_{20}(t)$ is the exit velocity at $x = 0^+$ of the downstream velocity field, u_2, in the jet. Downstream of the hole u_2 depends on time and space. In the jet we assume that capillarity is negligible, so that we can assume that the pressure is zero throughout the jet fluid. We could include the influence of gravity at this stage, but for this high-Froude -number flow the effect is only to bend the slender jet into an arc, whose radius of curvature is large compared with the diameter of the exit hole, and this has negligible upstream influence. See Vanden-Broeck and Keller [16] and Parau *et al.* [14].

Neglecting gravity, air resistance or any external force, each fluid element moves with a constant speed equal to that with which it leaves the exit hole:

$$u_2(t, \tau) = u_{20}(\tau), \tag{5}$$

where t is the current time and τ is the earlier time at which the fluid element left the exit hole: $0 \le \tau \le t$. At any current time, t, the jet is parameterised by τ, from $\tau = 0$ at the jet head, to $\tau = t$ for an element which is now leaving the exit at $x = 0^+$. Therefore the position of a material element of the jet is $x = X$, where

$$X(t, \tau) = (t - \tau)u_{20}(\tau). \tag{6}$$

Each material element of the jet has a varying cross-sectional area A_2, which changes so as to conserve the fluid volume between any two neighbouring material cross-sections in the jet. Suppose τ and $\tau + \delta\tau$ are parameter values that correspond to $x = X$ and $x = X + \delta X$, respectively, where $\delta\tau$ and δX have opposite sign. Then, at fixed time t, the volume of a material element of the jet can be written in three ways:

$$\int_\tau^{\tau+\delta\tau} A_{20}u_{20}(\tau)\,\mathrm{d}\tau = -\int_X^{X+\delta X} A_2(t, \tau)\,\mathrm{d}X = -\int_\tau^{\tau+\delta\tau} A_2(t, \tau)\frac{dX}{d\tau}\,\mathrm{d}\tau, \tag{7}$$

where $dX/d\tau$ is obtained from (6). Consequently the first and third integrals of (7) give us the time-dependent distribution of the jet's cross-sectional area:

$$A_2(t, \tau) = \frac{A_{20}}{1 - (t - \tau)\dot{u}_{20}(\tau)/u_{20}(\tau)}. \tag{8}$$

On the right-hand side of (8), we will find that $\dot{u}_{20}/u_{20} < 0$, so that A_2 is non-singular for all $t > 0$ and $\tau : 0 \le \tau \le t$.

For the jet, the above analysis with eqs (4–8) is equivalent to using the method of characteristics on the Eulerian partial differential equations of flow:

$$u_{2t} + u_2u_{2x} = 0 \qquad \text{and} \qquad A_{2t} + Au_{2x} = 0.$$

The characteristic curves in the x, t plane are straight lines. On each characteristic $u_2 =$ constant and A_2 decreases with increasing t. The slope of each characteristic is dictated by the speed $u_{20}(\tau)$ of the particle when it exited the hole at $x = 0$ at the earlier time τ. Importantly the characteristics do not intersect, because $u_{20}(\tau)$ decreases monotonically as τ increases. This view of the jet flow, from the theory of characteristics, shows us that our solution, in eqs (5, 6, 8), is valid throughout $x \ge 0$ and $t \ge 0$.

2.3. The coupling of the wave-water and jet flows

We now consider Bernoulli's equation in the wave water, and in the jet where the pressure p_2 is zero:

$$\frac{p_1}{\varrho} + \frac{\partial\phi_1}{\partial t} + \tfrac{1}{2}u_1^2 = f(t) = \frac{\partial\phi_2}{\partial t} + \tfrac{1}{2}u_2^2, \tag{9}$$

where $f(t)$ is a function shared by the regions 1 and 2 (because they share portions of the same streamlines) and ϕ_1 and ϕ_2 are the corresponding velocity potentials. In fact, for a thin barrier, we can write $\phi_1 = 0 = \phi_2$ at $x = 0$. We already know that $\phi_1 = xu_1(t)$ and so $\phi_{1t} = 0$ at $x = 0^-$. Similarly $\phi_{2t} = 0$ at $x = 0^+$. Hence at $x = 0$ (9) implies

$$\varrho^{-1}p_1(0,t) + \tfrac{1}{2}u_1(t)^2 = f(t) = \tfrac{1}{2}u_{20}(t)^2. \tag{10}$$

This completes the field equations. The initial conditions are $-\dot{L} = u_1 = u_{10}$, $L = L_0$ where L_0 and u_{10} are given positive constants, and the jet in region 2 starts from zero length. Our next task is to find $u_1(t)$, from which all the other flow variables follow. Before doing that in §3 we non-dimensionalise the variables and show that there is one parameter to describe the set of solutions.

2.4. Differential Equations of the Model and Non-dimensionalisation

Our starred dimensionless variables are defined as follows: time $t^* = t\,u_{10}/L_0$, coordinate $x^* = x/L_0$, length $L^*(t^*) = L(t)/L_0$, velocity $u_1^*(t^*) = u_1/u_{10}$, and pressure $p_1^* = p_1/(\varrho u_{10}^2)$. With respect to these we will solve the following coupled differential equations. Equation (3) becomes

$$p_1^*(x^*,t^*) = -(x^* + L^*)\frac{du_1^*}{dt^*}, \tag{11}$$

At $x^* = 0$ Bernoulli's Eq. (10) gives

$$p_1^*(0,t^*) + \tfrac{1}{2}u_1^*(t^*)^2 = f(t^*) = \tfrac{1}{2}u_{20}^*(t^*)^2, \tag{12}$$

the kinematic condition (1) at the rear of the wave water is

$$u_1^*(t^*) = -\frac{dL^*}{dt^*}, \tag{13}$$

and the volume-continuity condition for the whole fluid implies that

$$u_{20}^*(t^*) = \beta^{-1}u_1^*(t^*), \tag{14}$$

where $\beta = A_{20}/A_1$. The free surface shape is then

$$A_2^*(t^*,\tau^*) = \frac{\beta}{1 - (t^* - \tau^*)\dot{u}_{20}^*(\tau^*)/u_{20}^*(\tau^*)}. \tag{15}$$

Initially $u_1^* = L^* = -\dot{L}^* = 1$. Equations (11) and (15) contain just one parameter, β. In the next section we solve the initial-value problem.

3. Solutions in region 1: the wave-water flow

At $x = 0$ equations (11–14) give a differential equation for $L^*(t^*)$:

$$L^*\frac{d^2L^*}{dt^{*2}} = \alpha\left(\frac{dL^*}{dt^*}\right)^2, \tag{16}$$

where the constant $\alpha \geq 0$ is defined by

$$\alpha = \tfrac{1}{2}(\beta^{-2} - 1). \tag{17}$$

By using the identity $\ddot{L}^* = \dot{L}^* d\dot{L}^*/dL^*$ we reduce (16) from a second- to a first-order ordinary differential equation, and separate the variables. From this we obtain

$$\frac{dL^*}{dt^*} = -L^{*\alpha}.$$

Another separation of variables gives L^* as a function of t^*. The results depend on one parameter, α, and the distinct expressions for the class $\alpha \neq 1$ and the special case $\alpha = 1$ are as follows.

If $\alpha \neq 1$ then

$$L^*(t^*) = (1 + [\alpha - 1]t^*)^{1/(1-\alpha)}, \tag{18}$$

and from (13) the fluid velocity of the wave water is

$$u_1^*(t^*) = (1 + [\alpha - 1]t^*)^{\alpha/(1-\alpha)} \qquad \text{if,} \tag{19}$$

and from (11) the pressure distribution in $-L^* \leq x^* \leq 0$ is

$$p_1^*(x^*, t^*) = \alpha(x^* + L^*(t^*))(1 + [\alpha - 1]t^*)^{(2\alpha-1)/(1-\alpha)}. \tag{20}$$

If $\alpha = 1$ then

$$L^*(t^*) = \exp(-t^*), \tag{21}$$

$$u_1^*(t^*) = \exp(-t^*), \tag{22}$$

$$p_1^*(x^*, t^*) = (x^* + L^*(t^*)) \exp(-t^*). \tag{23}$$

The above dimensionless expressions are used to plot the results shown in Figs. 2–6.

In dimensional un-starred variables, the results correspond to the following expressions, which contain the initial speed u_{10} and length L_0 of the wave water.

If $\alpha \neq 1$ then

$$L(t) = L_0 \left(1 + [\alpha - 1]\frac{u_{10}}{L_0}t\right)^{1/(1-\alpha)}, \tag{24}$$

$$u_1(t) = u_{10} \left(1 + [\alpha - 1]\frac{u_{10}}{L_0}t\right)^{\alpha/(1-\alpha)}, \tag{25}$$

$$p_1(x, t) = \varrho u_{10}^2 \frac{\alpha}{L_0}(x + L(t)) \left(1 + [\alpha - 1]\frac{u_{10}}{L_0}t\right)^{(2\alpha-1)/(1-\alpha)}. \tag{26}$$

If $\alpha = 1$ then

$$L(t) = L_0 \exp(-u_{10}t/L_0), \tag{27}$$

$$u_1(t) = u_{10} \exp(-u_{10}t/L_0), \tag{28}$$

$$p_1(x, t) = \varrho u_{10}^2 L_0^{-1}(x + L(t)) \exp\left(-L_0^{-1}u_{10}t\right), \tag{29}$$

where α depends on the porosity β according to (17).

Figure 2 shows the wave water's velocity u_1^*, as a function of time after impact, for several values of β. The plot reveals two types of flow. First, for $\alpha \geq 1$ (or equivalently $0 \leq \beta \leq 3^{-1/2}$), the flow continues to slow down forever, because the low-porosity barrier retards the flow significantly. The second type of flow is for $0 \leq \alpha < 1$ (i.e. $3^{-1/2} < \beta \leq 1$), and the fluid flows relatively easily through the high-porosity barrier, and it does so in a finite time, T. For brevity in the following we define the critical value of β, that is the border between the two types of flow, as

$$\beta_c = 3^{-1/2} = 0.5774$$

to four significant digits.

From (24) we have $L = 0$ when $t = T$, where

$$T = \frac{2L_0\beta^2}{(3\beta^2 - 1)u_{10}} \qquad \text{if} \quad \beta_c < \beta \leq 1. \tag{30}$$

At time $t = T$ the last of the wave water reaches the hole and, simultaneously, the fluid velocity falls to zero. Hence at later times there is always fluid, at rest, in the hole: the rear of the jet is always connected to the hole as the jet stretches away. We discuss the flow and the shape of the jet in the next section. The spatial distribution of pressure has its highest value at $x = 0^-$. Equations (26, 29) imply that if $\beta \neq \beta_c$ then

$$p_1(0,t) = \tfrac{1}{2}\varrho u_{10}^2 \left(\frac{1}{\beta^2} - 1\right)\left(1 + \left[\frac{1}{\beta^2} - 3\right]\frac{u_{10}}{2L_0}t\right)^C, \tag{31}$$

where the power $C = 2(1 - \beta^2)/(3\beta^2 - 1)$, and if $\beta = \beta_c$ then

$$p_1(0,t) = \varrho u_{10}^2 \exp(-2u_{10}t/L_0). \tag{32}$$

Figure 3 shows the dimensionless pressure at the barrier, according to (31, 32), as a function of time for several values of β. At $t = 0^+$ the global maximum in pressure is

$$p_1(0^-, 0^+) = \tfrac{1}{2}\varrho u_{10}^2 \left(\frac{1}{\beta^2} - 1\right), \tag{33}$$

which shows that the global maximum in pressure is sensitivity to changes in β if β is small. The pressure is initially high for small values of β corresponding to a barrier that is nearly impermeable. In Fig. 3, the curve drawn for the smallest value, $\beta = 0.1$, has the highest initial pressure in the plot. In all cases the pressure decreases towards zero quickly after the initial maximum. In the Appendix the derivation of eq. (A3) makes clear that, for a short time before $t = 0$ in Fig. 3, the pressure rises very quickly from zero to precisely the pressure specified by (33) due to a brief violent flow that fills the hole.

Despite the rapid fluid deceleration that occurs for $\beta = 0.9$, near to $t = 1.13$ in Fig. 2, there is no corresponding spike in pressure in Fig. 3, because at that late time there is little mass (and hence little momentum) in the wave water. In Fig. 3, all the pressures fall to zero, or decline gradually towards zero, as t increases.

Following on from the ideas of Cooker and Peregrine [5], the pressure impulse on the outer face of the barrier is defined to be the time integral of the pressure during the impact. Ignoring the small impulse due to the brief rise in pressure discussed in Appendix A, the pressure impulse on the barrier is defined to be

$$I = \int_0^{T'} p_1(0^-, t)\,\mathrm{d}t, \tag{34}$$

where $T' = \infty$ if $0 \leq \beta < \beta_c$ or $T' = T$, equation (30), if $\beta_c \leq \beta \leq 1$.

In terms of β we find that

$$I(\beta) = \frac{1 - \beta^2}{1 + \beta^2}\varrho u_{10} L_0. \tag{35}$$

Expressions (34, 35) show that, although the maximum pressure (33) is singular in the limit $\beta \to 0$, the mechanically significant quantity of the pressure impulse remains bounded by the incident momentum $\varrho u_{10} L_0 A_1$ in this limit. Cooker and Peregrine [5] show that the pressure impulse is directly proportional to the change in fluid momentum. This is for the same reason that, in the elementary mechanics of a particle colliding with a

wall, the impulsive reaction of the wall can be equated with the particle's sudden change of momentum. For such an impact the impulse is the product of an indefinitely large force multiplied by an indefinitely small time of contact. Similarly the pressure impulse in a fluid is the product of an indefinitely large pressure multiplied by an indefinitely small time period of impact.

Returning to our discussion of the limit of small β, if the barrier is impermeable ($\beta = 0$) then (35) implies that all of the incident momentum, $\varrho u_{10} L_0$ per unit area of barrier, is destroyed by the impulsive reaction from the barrier. For an impermeable wall there is a tacit physical assumption that just after impact the fluid comes to rest (in the horizontal direction) *and remains in contact with the barrier*. However, the wave water could instantaneously bounce back from the barrier, with a coefficient of restitution $e : 0 < e \leq 1$. Such an impact would coincide with an even greater impulse on the barrier, $(1+e)\varrho u_{10} L_0$, which is up to twice that indicated by (35) with $\beta = 0$. See Wood and Peregrine [18] who modelled the bounce-back impact of a wave impacting on an impermeable wall.

At the other extreme, if the barrier is completely permeable ($\beta = 1$) then the fluid momentum is unchanged by the encounter, and (35) implies there is zero impulsive response from the barrier.

4. Solutions in region 2: the shape and flow of the jet

Equations (4–8) are the solution for the jet, written parametrically in terms of $u_{20}(\tau)$, which in turn only depends on $u_1(\tau)$, given explicitly by (25, 28). Equation (15) implies that

$$A_2^*(t^*, \tau^*) = \frac{\beta(1 + [\alpha - 1]\tau^*)}{1 + \alpha t^* - \tau^*}. \tag{36}$$

Figure 4 shows results for the cross-sectional area of the jet for $\beta = 0.8$, a value high enough that the fluid flows through the barrier in a finite time $T^* = 1.391$. Thereafter the material fluid element at the exit, $x = 0^+$, has zero speed and the jet's cross-sectional area there falls to zero for $t^* > T^*$. Each material element of the jet moves at its own constant distinctive speed; the jet lengthens and thins everywhere. The jet head also thins over time, but, for this sufficiently large value of β, it is the head that remains the *thickest* cross-section of the jet.

Figure 5 shows a jet from the other class of flow, when β is small. This example is for $\beta = 5^{-1/2} = 0.4472$ ($\alpha = 2$), a value of β less than the critical value $\beta_c = 0.5774$. Here the decelerating fluid in the wave takes forever to flow through the barrier. As before, each element of the jet moves with its own distinctive speed, and the jet lengthens and thins everywhere. The jet head remains the *thinnest* section of the jet. From (15) we see that, as t^* tends to infinity, the thickness for every cross-section decreases as t^{*-1}. For a jet that is in the form of a sheet, eqs (4) and (36) ensure that the thickness of the jet decreases to zero algebraically, with increasing x^*, as t^* tends to infinity. Similarly, for a jet which is axisymmetric with circular cross-sections, eqs (4) and (36) ensure that the radius of each material cross-section decreases as $t^{*-1/2}$ as t^* tends to infinity.

The Lagrangian description of the jet fluid velocity, $u_2(t, \tau) = u_{20}(\tau)$, can be re-expressed in an Eulerian framework as discussed at the end of section 2.2. Qualitatively the continual deceleration of the wave water ensures that $u_{20}(\tau)$ is a monotone decreasing function. Hence the field of velocity in the jet ensures that the fluid domain is everywhere continually being lengthened by faster fluid moving ahead of slower fluid. Figure 6 shows the spatial distribution of velocity at time $t^* = 1.0$, which corresponds to the last profile drawn in Fig. 5. The distribution is close to linear. The cross-sectional area of each fluid

element of the jet continually decreases in time as compensation for the longitudinal spreading of the liquid, which in turn is due to the spatial gradient in the fluid velocity.

Finally we show that after the fluid has penetrated the barrier there is no energy loss. The fluid energy is all kinetic: before impact the kinetic energy is $\mathrm{KE}_1 = \frac{1}{2}\varrho u_{10}^2 L_0 A_1$. On the other side of the barrier we can obtain the downstream kinetic energy KE_2 by integrating (over a sufficiently long period of time) the kinetic energy flux $1/2\varrho u_{20}^3 A_{20}$ at the exit of the hole. Here $u_{20}(t)$ is given by (25, 28). The calculation implies that the downstream kinetic energy is $\mathrm{KE}_2 = \frac{1}{2}\varrho u_{10}^2 L_0 A_1$. Hence $\mathrm{KE}_2 = \mathrm{KE}_1$ for $0 < \beta \leq 1$. So while penetrating the barrier there is no kinetic energy loss. This is as we would expect on physical grounds, as the flow is frictionless and the fixed barrier can do no work on the fluid.

5. Example calculation

We now put in context the magnitude and duration of the pressure predicted by (32). Suppose water from a breaking wave presents a thickness $L_0 = 1\mathrm{m}$, moving with a speed of the order of $\sqrt{gL_0}$, hence we can take $u_{10} = 3\mathrm{m/s}$. Let the impact be onto a wall of porosity $\beta = 0.1$, and surface layer width $W = 0.1\,\mathrm{m}$. Then over the short time of 0.018 seconds the pressure at the barrier rises to a global maximum that is nearly $150{,}000\,\mathrm{N/m^2}$. This is a peak pressure that is 1.5 times atmospheric pressure. It is within the range of impact pressures computed, measured and reviewed by Bredmose *et al.* [4]. Using L_0 as our suitable length scale, the results of Bredmose *et al.* suggest that peak pressures lie between ten and twenty $\varrho g L_0$.

From Fig. 3 we see that the time scale for the impact pressure to decay to $1\,\mathrm{N/m^2}$ is just $0.12\,L_0/u_{10} = 0.04$ seconds. From Fig. 2, we find that with $\beta = 0.1$ the incident flow speed, u_1, decelerates over this time from 3m/s to 0.3m/s, and the head of the jet exits the hole with initial speed 30m/s. By the time $t = 0.04$ seconds, the jet is 1.5m long, and is therefore already longer than the incident wave water. If the jet is unimpeded in its flight, the jet head stays the thinnest section and continues to travel at $30\,\mathrm{m/s}$. Meanwhile at the hole, the jet water is now moving at only $0.09\,\mathrm{m/s}$.

According to eq (35) the impulse, I, on the barrier is 98% of the theoretical maximum value of $\varrho u_{10} L_0 = 3000\,\mathrm{Ns/m^2}$, which would be experienced by an impermeable wall. To put this in context, such a pressure impulse is similar in size to that delivered by a wrecking ball, whose momentum per unit area of collision is mv/A. Suppose a steel ball of mass $m = 1000\,\mathrm{kg}$ impacts masonry over one hemisphere of contact area $A = 0.8\mathrm{m}^2$, and suppose the incident speed is a moderate $v = 2.4\,\mathrm{m/s}$. Then the average pressure impulse over the hemisphere of contact between the steel ball and the masonry is $mv/A = 3000\,\mathrm{Ns/m^2}$, the same as that from our example wave.

6. Discussion, conclusions and further work

The model presented is simple enough to capture the essential fluid dynamics in one spatial dimension. The impact pressure quickly rises to a peak and then falls. The peak impact pressure is $\frac{1}{2}\varrho u_{10}^2(\beta^{-2} - 1)$. For small β the pressure decreases quickly, and the pressure impulse is finite, even when $\beta = 0$ and the pressure is unbounded: see Fig. 3 and (35).

The results fall into two classes, depending on the porosity β. If the barrier has a small enough porosity ($\beta < \beta_c$) then the wave water takes forever to slow down to rest. Alternatively, if the barrier has a high enough porosity ($\beta \geq \beta_c$), then all of the wave water

reaches the exit hole in a finite time, T that decreases to L_0/u_{10} as β increases to unity. At $t = T$ the last fluid element in the wave water reaches the hole and is simultaneously brought to rest at the exit. An experimental investigation would reveal whether barriers of differing permeability produce qualitatively different flows either side of a critical porosity β_c. Photographic evidence might confirm the theory's prediction that the jet is thin-headed for low permeabilities $\beta < \beta_c$ and fat-headed for high-porosity barriers, $\beta \geq \beta_c$. As time increases the jet thins everywhere, due to the velocity gradient in the jet.

While the fluid penetrates the barrier there is no energy loss.

We have assumed that the jet velocity when exiting the hole is primarily in the direction **i**, which points at right angles into the breakwater. This is reasonable when the hole has some line or axis of symmetry parallel to the x-axis. Otherwise the hole would be able to exert a non-zero force orthogonal to the direction **i**. Such a force would deflect the stream into some fixed direction indicated by a unit-vector **d**, different from direction **i**. Such a jet flow could be accommodated by interpreting our results for the longitudinal velocity u_2 and the cross-sectional area A_2 with respect to the jet axis of **d**.

The analysis rests on the assumption that fluid regions 1 and 2 are connected through the hole. Are there circumstances under which the fluid could 'bounce' from the barrier on initial impact? Could the flow spontaneously sever the connection through the hole, during the fluid deceleration on the seaward side? A bubble or a rough-edged hole might induce ventilation that could promote a separation of the two fluid regions.

Further work is needed on the three-dimensional flow: the incident wave water may not flow normal to the wall, or the impacting wave water may not have constant thickness L_0, and it could strike with a spatially non-uniform normal velocity component u_{10}. That said, a wave approaching at normal incidence is the most interesting to treat as it coincides with the highest impact pressures, although a component of fluid velocity parallel to the barrier could be included. If our model parameters are functions $L_0(y, z), \beta(y, z), u_{10}(y, z)$ or $\beta(y, z)$ that vary sufficiently slowly with respect to the (y, z) coordinates, then we could accommodate jets whose properties have correspondingly slow variations in y and z. In other words any one jet depends only on the *local* conditions of impact seaward of its hole. For an inhomogeneous array of holes, it would be worth further investigation to identify the control volume of fluid in the wave that supplies fluid to each hole.

Appendix A

Our aim is to model the quick rise in pressure while the front of the wave penetrates the barrier, and to show that this pressure rise-time is so short that we can dismiss the hole penetration phase of the flow from the dynamics of the system modelled in the current paper.

In Fig. 1 the wave water first makes contact with the barrier at the left-hand vertices of the triangles, which in pairs form the entrance to each hole. We suppose that the forward face of the wave is a free surface, at $x = F(t)$, at which the pressure p is zero. The free surface advances through the narrowing hole. We suppose that the velocity of the rear of the wave water is maintained at its initial value u_{10} throughout the short time that the forward free surface takes to traverse the hole from $x = -W$ to $x = 0$. The constant W is the length of the hole, and $W \ll L_0$. (If we were to allow u_1 to decrease from u_{10} during the flow described here, then this would only *reduce* the pressure from that found below.)

Suppose, without loss of generality, that the cross-sectional area of the hole varies *linearly* with x between A_1 at $x = -W$ and A_{20} at $x = 0$. Hence the cross-sectional area is

$$A(x) = A_1 - \frac{x + W}{W} (A_1 - A_{20})$$

(If the hole is also axisymmetric then the hole is a truncated section of a parabola of revolution.) We know that the fluid volume flux at the entrance to the hole, at $x = -W$, is the product of the speed u_{10} and the cross-sectional area A_1. This volume flux equals that at the free surface $x = F$, where the fluid speed is dF/dt and the cross-sectional area is $A_1 - W^{-1}(F + W)(A_1 - A_{20})$). Equating these volume fluxes gives us

$$\frac{dF}{dt} = \frac{u_{10}}{\beta - F(t)W^{-1}(1-\beta)}, \tag{A1}$$

where $\beta = A_{20}/A_1$. Since the volume flux through every cross-section of the hole is the same, we can write down the Eulerian fluid velocity, u, in the hole:

$$u(x) = \frac{u_{10}}{\beta - xW^{-1}(1-\beta)} \qquad -W \le x \le F(t). \tag{A2}$$

Note that in (A2) $u(x)$ does not depend on t during the time that the forward free surface is advancing within the hole. Expression (A2) is in accord with the kinematic condition $dF/dt = u(F)$ at $x = F(t)$.

The pressure distribution $p(x, t)$ in the hole comes from Bernoulli's equation: for $x : -W \le x \le F(t)$ we have

$$p(x,t) = \tfrac{1}{2}\varrho u(F)^2 - \tfrac{1}{2}\varrho u(x)^2. \tag{A3}$$

According to (A3) the pressure rises in time at every point as F increases from $-W$ to 0. The RHS of (A3) is the difference between two squares. So the highest pressure occurs *when* the first term is largest (when $F = 0$), and simultaneously *where* the second term in (A2) is smallest (at $x = -W$). This maximum pressure we name $p_{\max} = \frac{1}{2}\varrho u_{10}^2(\beta^{-2} - 1)$, and it coincides with the pressure at $t = 0^+$ (equation 33) in Fig. 3.

The time t_s for the pressure to rise from zero to this maximum can be obtained from separating the variables and integrating (A1) from $F = -W$ to $F = 0$ and from $t = 0$ to $t = t_s$. We find that

$$t_s = \tfrac{1}{2}(1+\beta)\frac{W}{u_{10}}, \tag{A4}$$

which also equals the volume of the hole divided by the constant fluid volume flux through it. The coefficient one-half at the front of expression (A4) only depends on how the cross-sectional area of the hole changes with distance. Here it is linear, so that the hole is a volume of revolution of an arc of a paraboloid. For a right-circular conical hole the first coefficient of (*A*4) is instead one-third.

Since $W \ll L_0$, (A4) implies that the initial transients in the flow, created while the wave is first encountering the barrier, occur over a time scale t_s that is much shorter than the time scale L_0/u_{10} on which events occur in §2 of the current paper. For each curve in Fig. 3 we can suppose that the initial highest pressure is reached very quickly over a small time interval before $t = 0$ in the plot. Therefore we can neglect the details of the flow inside the hole and reduce its width to a transition between $x = 0^-$ and $x = 0^+$ in §2. We can also ignore the contribution to the impulse due to this phase of the flow while the pressure is increasing, because it is a small fraction W/L_0 times the initial momentum $\varrho u_{10} L_0$ discussed in and after (35).

Acknowledgments: The author thanks the anonymous referees for their work in commenting helpfully on an earlier version of this article.

References

1. Bagnold, R.A. 1939 Interim report on wave pressure research. *Proc. Inst. Civ. Eng.* **12**, 201–226.
2. Birkhoff, G., MacDougall, D.P., Pugh, E.M. & Taylor, G.I. 1948 Explosives with lined cavities. *J. Applied Physics* **19**, 563–582.
3. Birkhoff, G. & Zarantonello, E.H. 1957 *Jets Wakes and Cavities*. Academic, New York.
4. Bredmose, H., Hunt-Raby, A, Jayaratne, R. & Bullock, G.N. 2010 The ideal flip-through impact: experimental and numerical investigation. *J. Eng. Math.* **67**, 115–136.
5. Cooker, M.J. & Peregrine, D. H. 1995 Pressure-impulse theory for liquid impact problems. *J. Fluid Mech.* **297**, 193–214.
6. Cooker, M.J. 2002 Unsteady pressure fields which precede the launch of free surface liquid jets. *Proc. R. Soc. Lond.* **A458**, 473–488.
7. Cooker, M.J. 2010 The flip-through of a plane inviscid jet. *J. Eng. Math.* **67**, 137–152.
8. Faltinsen, O. 1993 Sea Loads on Ships and Offshore Structures. Cambridge University Press.
9. Howison, S.D., Ockendon, J.R. & Wilson, S.K. 1993 Incompressible water-entry problems at small deadrise angles. *J. Fluid Mech.* **222**, 215–230.
10. Howison, S.D., Ockendon, J.R., Oliver, J., Purvis, R. & Smith, F.T. 2005 Droplet impact on a thin fluid layer. *J. Fluid Mech.* **542**, 1–23.
11. King, A.C. & Needham, D.J. 1994 The initial development of a jet caused by fluid, body and free-surface interaction. I. A uniformly accelerating plate. *J. Fluid Mech.* **268**, 89–101.
12. Korobkin, A. A. & Yilmaz, O. 2009 The initial stage of the dam-break problem. *J. Eng. Math.* **63**, 293–308.
13. Needham, D.J., Chamberlain, R. & Billingham, J. 2008 The initial development of a jet caused by fluid, body and free-surface interaction. Part 3. An inclined accelerating plate. *Quart. Journal of Mechanics & Applied Mathematics* **61**, 581–614.
14. Parau, E.I., Decent, S.P., Simmons, M.J.H., Wong, D.C.Y. & King, A.C. 2007 Nonlinear viscous liquid jets from a rotating orifice. *J. Eng. Math.* **57**, 159–179.
15. Taylor, G. I. 1943 A formulation of Mr. Tuck's conception of Munroe jets. In *The Scientific Papers of Sir Geoffrey Ingram Taylor* (ed. G.K. Batchelor). Volume 3, 358–362.
16. Vanden-Broeck, J-M. & Keller, J.B. 1982 Jets rising and falling under gravity. *J. Fluid Mech.* **124**, 335–345.
17. Wagner, H. 1932 Gleitvorgange an der oberflache von flussigkeiten. *Zeitschrift fur Angewandte Mathematik und Mechanik* **12**, 193–215.
18. Wood, D.J. & Peregrine, D.H. 2000 Wave impact on a wall using pressure impulse theory: 2. porous berm. *J. Waterway Coastal & Ocean Eng. Div. ASCE.* **126**, (4), 191–195.

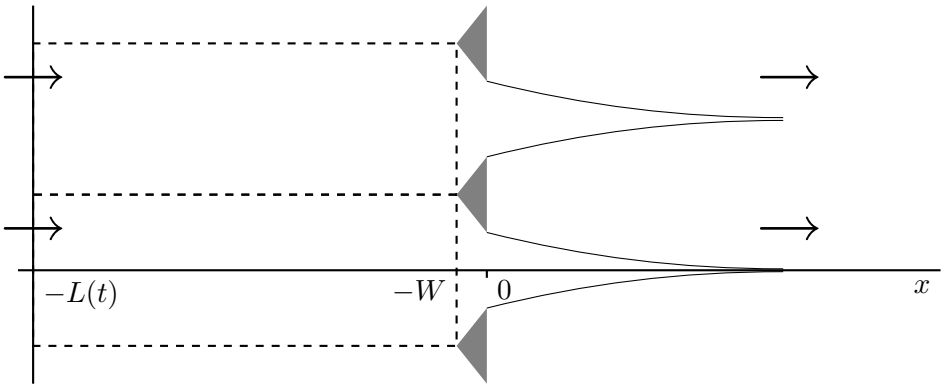

Figure 1. Sketch of the horizontal flow through the thin barrier $-W < x < 0$. In the interval $-L(t) < x < -W$ the wave water moves to the right against the barrier, and free jets flow to the right into $x > 0$. The arrangement is periodic in the directions normal to the x-axis. Each dashed rectangular region in $-L < x < 0$ is the outline of a control volume between the vertical free surface at the left and the barrier. For each fixed x, this control volume has cross-sectional area A_1.

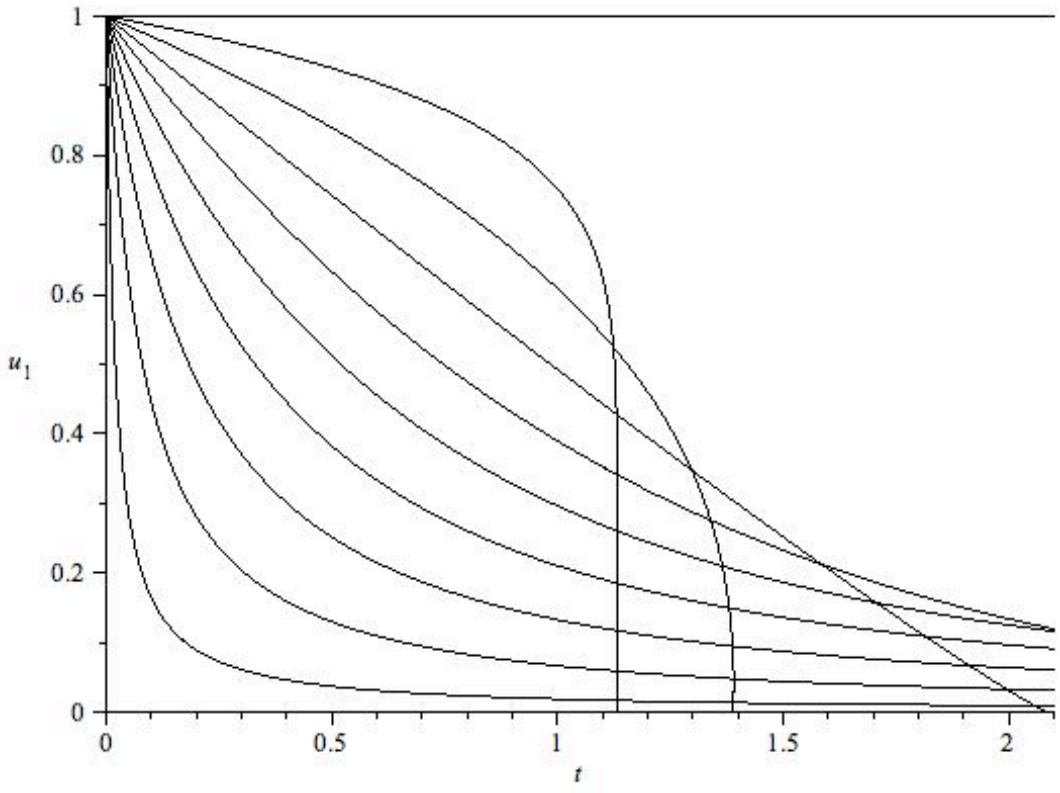

Figure 2. Time dependence of the dimensionless wave water velocity $u_1^*(t^*)$. Curves drawn for $\beta = 0.1, 0.2, ..., 1.0$. The lowest curve drawn is for $\beta = 0.1$; the uppermost line, $u_1 = 1$, is for $\beta = 1$.

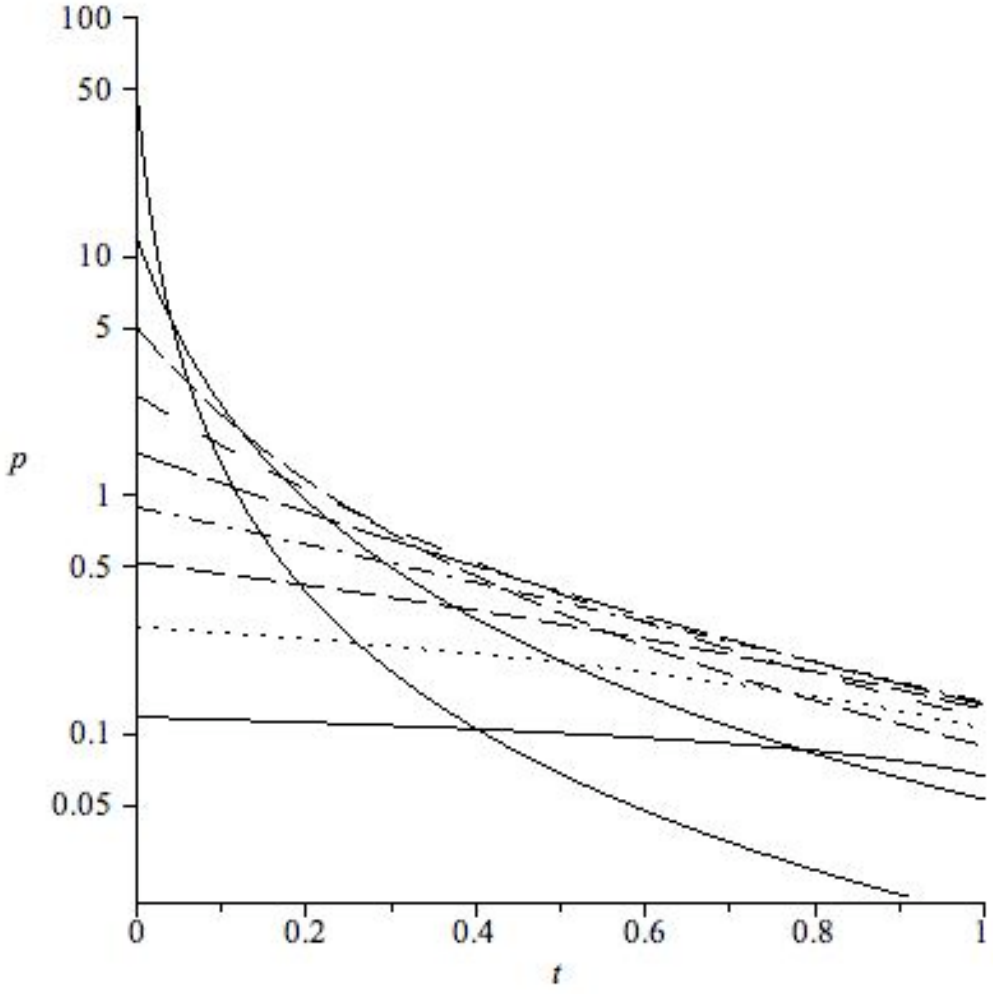

Figure 3. The dimensionless pressure eq. (20) at the barrier $x^* = 0^-$, as a function of t^*. The vertical scale is logarithmic. See also eq. (31). The curves are drawn for $\beta = 0.1, 0.2, ..., 0.9$. The highest initial pressure is for $\beta = 0.1$. The lowest initial pressure is for $\beta = 0.9$.

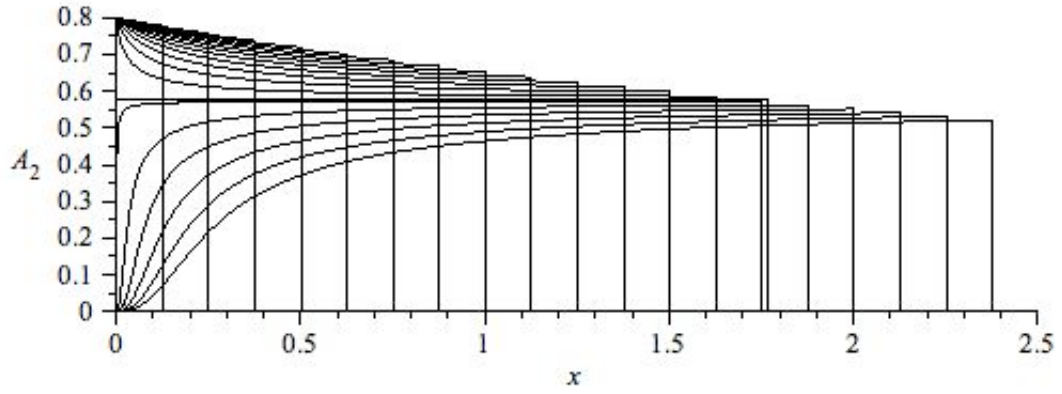

Figure 4. The dimensionless cross-sectional area A_2^* of the jet as a function of x^* at several instants. The flow is from left to right as t^* increases. Drawn for $t^* = 0.1, 0.2, ..., 1.9$. Here $\beta = 0.8 > \beta_c$. At $x^* = 0^+$ the jet tail's speed and thickness fall to zero at $t^* = T = 1.391$, also drawn. At $t^* = T$ all the fluid is in the jet. For $t^* > T$ the head is the widest cross-section of the jet.

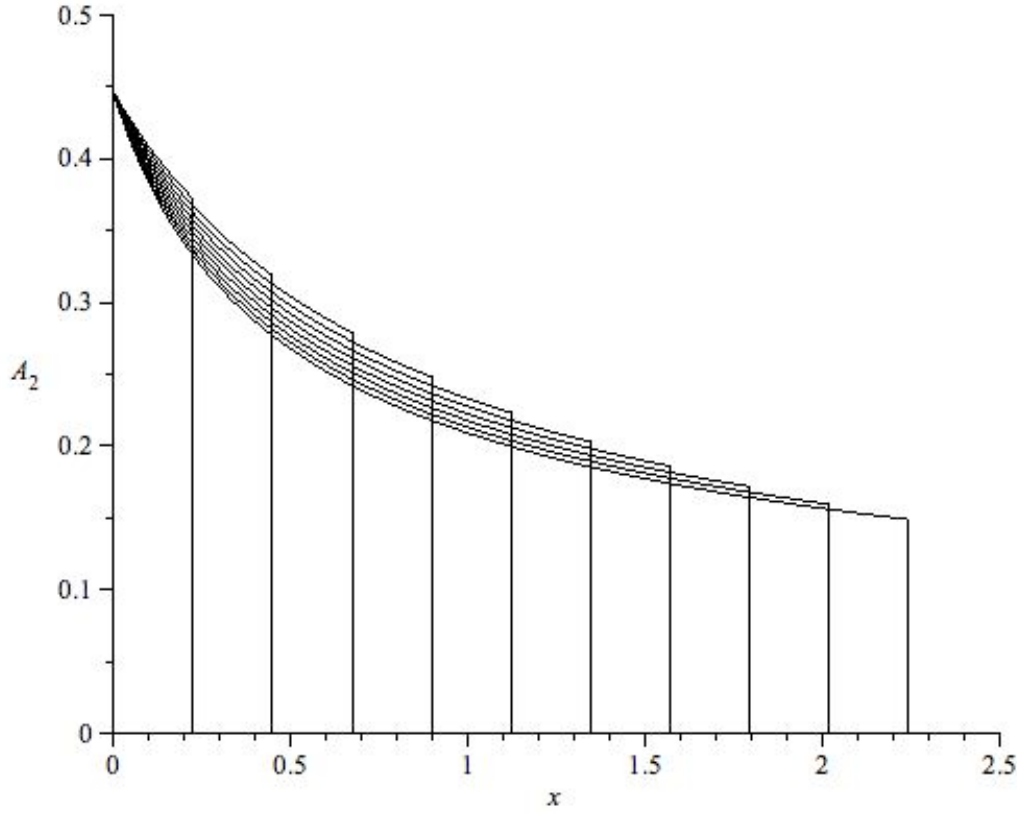

Figure 5. The cross-sectional area A_2^* of the jet as a function of x^* at several instants, for $\beta = 0.4472 < \beta_c$. The flow is from left to right as t^* increases. Drawn for $t^* = 0.1, 0.2, ..., 1.0$.

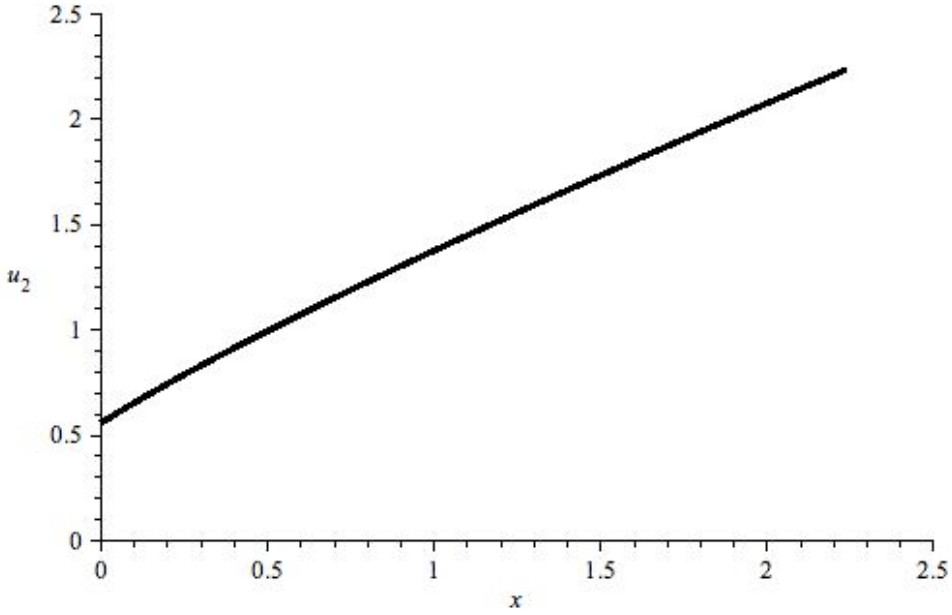

Figure 6. The spatial distribution of velocity in the jet corresponding to the last time $t^* = 1.0$ shown in Fig. 5, for $\beta = 0.4472 < \beta_c$.